

First-Principles Studies of Three Pristine and BN-Doped Graphyne Allotropes

Q. WEI^{a,*}, Q. WANG^a, X. XIE^a, X. JIA^a, Z. WU^a,
H. YAN^b, M. ZHANG^c, M. HU^a AND X. ZHU^d

^a*School of Physics, Xidian University, 710071 Xi'an, China*

^b*College of Chemistry and Chemical Engineering, Baoji University of Arts and Sciences, 721016 Baoji, China*

^c*College of Physics and Optoelectronic Technology, Baoji University of Arts and Sciences, 721016 Baoji, China*

^d*School of Information, Guizhou University of Finance and Economics, 550025 Guiyang, China*

Received: 01.06.2023 & Accepted: 21.11.2023

Doi: [10.12693/APhysPolA.145.71](https://doi.org/10.12693/APhysPolA.145.71)

*e-mail: qunwei@xidian.edu.cn

The electrical and electronic characteristics of three graphyne allotropes (10-18-6 graphyne, 10-12-18-6 graphyne, and 12-14-18-6 graphyne) were examined based on first-principles calculations using the generalized gradient approximation. The changes in system characteristics when carbon atoms were replaced with boron and nitrogen atoms were thoroughly investigated. The findings demonstrate that the positions of the doping atoms are strongly related to the band gap of doped graphyne. Meanwhile, band structure calculations also clearly reveal that the band gap can be adjusted via BN doping. The ability to regulate the band gap will increase the likelihood of the broad usage of these allotropes in nanoelectronic devices.

topics: graphyne, electronic properties, BN-doped, first-principles calculations

1. Introduction

Due to its various hybridization states, carbon can form a wide variety of allotropes [1–5] with various properties and dimensions, including three-dimensional (3D) diamond and graphite, two-dimensional (2D) graphene [6] and graphynes [7], the one-dimensional (1D) nanotubes [8], and the zero-dimensional (0D) fullerenes. With the successful fabrication of graphene, two-dimensional (2D) carbon materials have also received much attention [9–11]. Despite the fact that graphene exhibits intriguing features such as high electron mobility [12, 13] and Dirac cones [14], the great drawback of a zero band gap severely restricts the direct applicability of graphene in electrical devices such as diodes [15] and digital transistors. To be acceptable for nanoelectronic applications, the band gap quality of graphene must be appropriately adjusted in some way, which has been investigated through a number of methods [16–20]. Using these methods, it has been discovered, among other things, that alternating boron (B) and nitrogen (N) atom doping has a favourable effect on graphene band gap tuning [19]. First, B and N are neighbours of carbon (C)

on the periodic table, which means that their atomic radii are quite close to that of C. Second, doping with B and N causes graphene to change from a semimetal to a semiconductor, potentially opening up more opportunities for its use in nanoelectronic devices. B and N codoping can adjust the band gap of graphene nanosheets [18–20]. The band gap of the BCN material produced after adding B and N atoms to graphene changes depending on the doping concentration [21–23]. For instance, the work by Zhang et al. [22] showed that altering the carbon concentration can be used to adjust the band gap of hybrid graphene-like BCN nanosheets.

A novel two-dimensional carbon allotrope called graphyne was first proposed by Baughman et al. [24] and is typically characterized by Dirac cones [25] with hexagonal rings connected by acetylenic bonds. Due to the existence of acetylenic bonds, the adjustment of the structure of graphyne is more flexible. Unlike graphene, because of the presence of acetylenic bonds, neither graphyne nor members of its family have a zero band gap, which may provide excellent opportunities for their use in electronic devices. However, due to the small band gap of graphyne and members of its family,

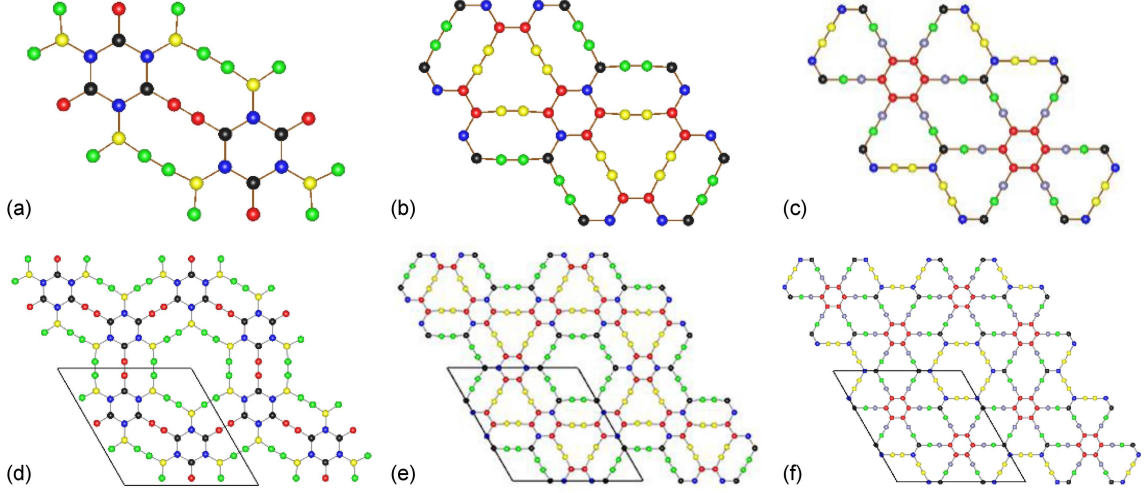


Fig. 1. Primitive cells of (a) 10-18-6 graphyne, (b) 10-12-18-6 graphyne, and (c) 12-14-18-6 graphyne, and $2 \times 2 \times 1$ supercells of (d) 10-18-6 graphyne, (e) 10-12-18-6 graphyne, and (f) 12-14-18-6 graphyne.

the widening of the band gap is needed for electronic devices [26]. Graphyne has higher flexibility than graphene and carbon nanotubes due to the capacity to adjust its band gap by varying the size of the hexagonal ring and the length of the chain. In addition, the acetylenic bonds in graphyne make tuning its band gap by codoping BN atoms at different positions more flexible compared to graphene [27–34]. Deng et al. [28, 29] observed, for example, that the band gaps of α -graphyne and γ -graphyne are altered on a regular basis when the distance between the dopant B and N atoms increases. Mu and Li [30] discovered that when sp and sp^2 carbon pairs are substituted by BN pairs, the effects on β -graphyne are different, and the resulting structures are semi-metallic and wide-band-gap structures, respectively. Band gap opening can be induced by doping a BN pair in the unit cell of 6,6,12-graphyne, as demonstrated by the work of Malko et al. [31]. Further investigation revealed that the band gap of 6,6,12-graphyne exhibits an odd-even effect when the BN codoping concentration gradually rises [32]. Notably, Bhattacharya et al. [33] reported that the band gap of γ -graphyne derivatives is modulated from infrared to ultraviolet (UV) via the visible region due to the presence of BN at separate locations.

Due to the successful synthesis of BN-doped graphene and BN sheets [21, 35], two-dimensional carbon materials have drawn much attention. In this study, we explore all BN substitution scenarios for three graphyne allotropes. We first investigate structures in which BN replaces carbon atoms in the hexagonal ring, then structures in which BN replaces carbon atoms in the linear chain, and last, structures in which all carbon atoms are replaced by BN atoms. The impact of BN substitution at different positions on the electronic structure and associated parameters, such as the partial density of states, is investigated here.

2. Calculation methods

Under the framework of density functional theory (DFT) [36, 37], calculations of the pertinent characteristics were performed using the Vienna *ab initio* simulation program (VASP) [38] and the projected augmented wave method [39, 40]. To eliminate interlayer interactions, a vacuum layer of 20 Å was created along the z -axis direction. The generalized gradient approximation (GGA) proposed by Perdew, Burke, and Ernzerhof (PBE) [41] was used for the exchange–correlation functional. A plane wave was chosen for the electronic wave function expansion basis set, and the cut-off energy was eventually chosen to be 500 eV after multiple convergence tests. For 10-18-6 graphyne, 10-12-18-6 graphyne, and 12-14-18-6 graphyne, $3 \times 3 \times 1$, $3 \times 3 \times 1$, and $2 \times 2 \times 1$ Monkhorst–Pack k -point meshes [42] were used for Brillouin zone integration, respectively. The geometry was optimized using convergence criteria for electron self-consistent relaxation and ionic relaxation, and the energy and force criteria were set to 1×10^{-5} eV and 0.001 eV/Å, respectively.

3. Results and discussion

The optimized structures of the three graphyne allotropes are displayed in Fig. 1. As shown in Fig. 1a–c, the primitive cell of 10-18-6 graphyne contains 36 carbon atoms, while the primitive cells of 10-12-18-6 graphyne and 12-14-18-6 graphyne contain 48 and 60 atoms, respectively. The optimized lattice constants are 11.98 Å, 13.81 Å, and 16.37 Å, in agreement with the literature (11.99 Å, 13.81 Å, and 16.38 Å) [43]. Both 10-18-6 graphyne and 10-12-18-6 graphyne have five different types of nonequivalent carbon atoms, unlike graphyne and

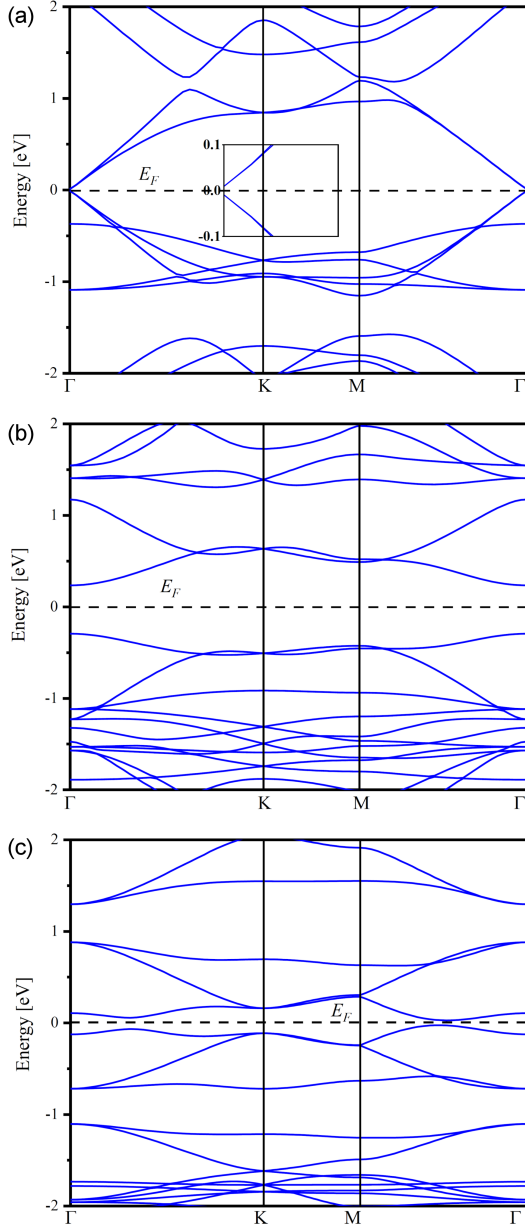


Fig. 2. Band structure of (a) 10-18-6 graphyne, (b) 10-12-18-6 graphyne, and (c) 12-14-18-6 graphyne.

graphdiyne. The five unequal C1, C2, C3, C4, and C5 atoms are represented by black, blue, red, green, and yellow spheres, respectively, to make separating them easier. For 10-18-6 graphyne, C1, C2, and C5 are sp^2 -hybridized atoms, and C3 and C4 are sp -hybridized atoms. For 10-12-18-6 graphyne, C1, C2, and C3 are sp^2 -hybridized atoms, while C4 and C5 are sp -hybridized atoms. In contrast, 12-14-18-6 graphyne contains six types of carbon atoms, C1, C2, C3, C4, C5, and C6, which are represented by black (C1), blue (C2), red (C3), green (C4), yellow (C5), and grey (C6) spheres. C1, C2, and C3 are sp^2 -hybridized carbon atoms, while C4, C5, and C6 are two-coordinated (sp -hybridized) carbon atoms.

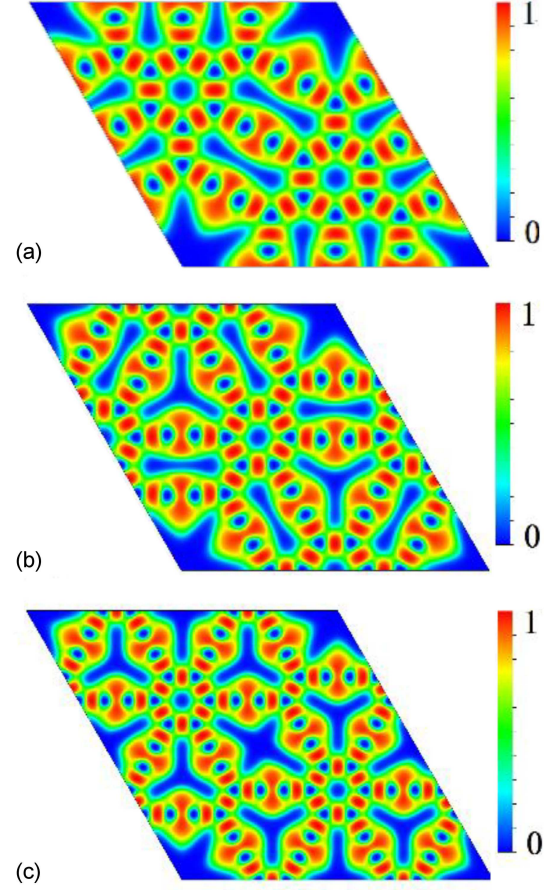


Fig. 3. Calculated ELF of (a) 10-18-6 graphyne, (b) 10-12-18-6 graphyne, (c) 12-14-18-6 graphyne.

It can be seen in Fig. 1d–f that 10-18-6 graphyne is composed of 10-atom, 18-atom and 6-atom rings, while 10-12-18-6 graphyne is composed of 10-atom, 12-atom, 18-atom, and 6-atom rings, and 12-14-18-6 graphyne is composed of 12-atom, 14-atom, 18-atom, and 6-atom rings.

As illustrated in Fig. 2a, pristine 10-18-6 graphyne is a direct band gap semiconductor with a band gap value of only 0.018 eV, and its conduction band minimum (CBM) and valence band maximum (VBM) are both located at the Γ point. The band structure of 10-12-18-6 graphyne is shown in Fig. 2b and is similar to that of 10-18-6 graphyne, reflecting a direct band gap semiconductor with a band gap of only 0.528 eV. CBM and VBM are also located at the Γ point. Compared to 10-18-6 graphyne, 10-12-18-6 graphyne has a higher band gap. The band structure of 12-14-18-6, as shown in Fig. 2c, demonstrates that it is also a direct band gap semiconductor with a band gap of 0.053 eV and that CBM and VBM are situated between the M point and Γ point. Additionally, we simultaneously estimated the electron localization function (ELF) to better understand the bonding characteristics of pristine 10-18-6 graphyne, as shown in Fig. 3a and c. The value of ELF ranges from 0.0 to 1.0, where 1.0 and

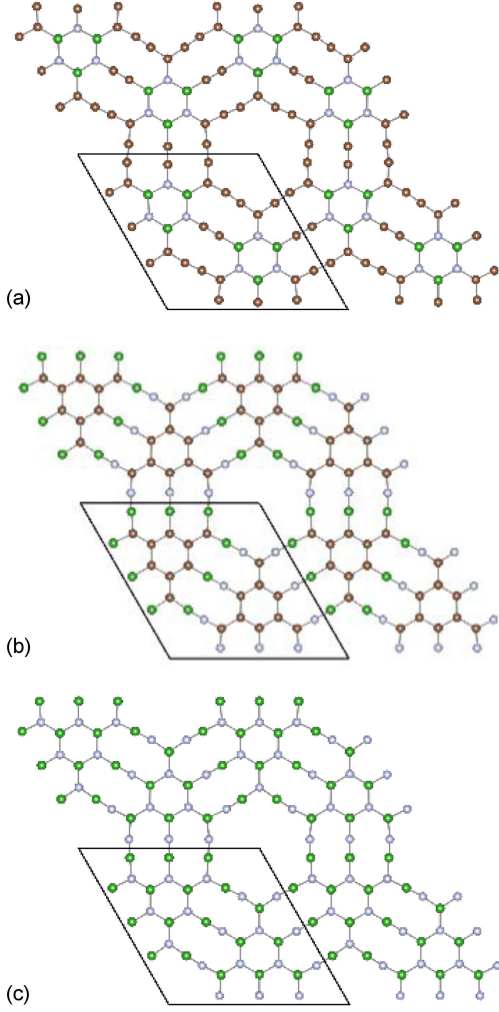


Fig. 4. Optimized structures of (a) 10-18-6 graphyne with BN in the hexagonal ring, (b) 10-18-6 graphyne with BN in the linear chain, and (c) 10-18-6 graphyne-like BN sheet.

0.5 indicate that the electrons are in a highly localized state and a highly delocalized state, respectively. The system electrons are entirely concentrated between the carbon-carbon bonds, as seen in Fig. 3a-c, and the ELF value of 0.8 suggests a high level of electron localization.

Figure 4a and b displays two derivatives of 10-18-6 graphyne that have been doped with boron and nitrogen atoms. The first structure is composed of BN hexagonal rings connected by carbon chains made by replacing carbon atoms in the hexagonal ring, while the second structure is composed of carbon hexagonal rings connected by BN chains made by replacing atoms in the carbon chain. Figure 4c depicts the graphyne-like “BN sheet” created when B and N atoms are alternately placed in place of all carbon atoms in pristine 10-18-6 graphyne. In general, for the three pristine graphyne allotropes, the system formed by replacing carbon atoms between two carbon hexagonal rings with alternating

TABLE I

Lattice constants (in Å) of 10-18-6 graphyne, 10-12-18-6 graphyne, and 12-14-18-6 graphyne.

	Pristine	Systems with BN		BN sheet
		at hex. ring	at linear chain	
10-18-6 graphyne	11.98	12.11	12.10	12.21
10-12-18-6 graphyne	13.81	13.97	13.93	14.05
12-14-18-6 graphyne	16.37	16.47	16.57	16.66

arrangements of boron and nitrogen is referred to as the “system with BN in the linear chain”, while the replacement of all carbon atoms of the original carbon hexagonal ring forms the “system with BN in the hexagonal ring”. Finally, we generated the “BN sheet” by completely replacing all of the carbon atoms in pure graphyne with alternate combinations of boron and nitrogen.

The lattice constants of the three new systems are shown in Table I. Considering a single pristine graphyne, doping at different positions will cause the lattice constant of the new system to change. This is due to the difference in the atomic radii of the boron, carbon, and nitrogen atoms, as well as the difference in the types of chemical bonds formed at different positions. Overall, after codoping with B and N atoms, the lattice constant increases, and the BN sheet has the largest lattice constant.

We have numbered all the types of bonds in the original structures for better elaboration, as shown in Fig. 5. In this research, we discovered that the length of the C-C bond (bond 1) of the hexagonal ring in 10-18-6 graphyne between two sp^2 -hybridized C atoms is 1.45 Å, which is between the values for a single bond (~ 1.47 Å) and a double bond (~ 1.38 Å). The σ bonds are composed of p_x , p_y , and s orbitals, and π bonds are composed of p_z orbitals. Therefore, this hexagonal ring has the π -conjugated characteristic of graphyne. A π bond exists between the hexagonal ring and the C chain because bonds 2 and 4 are 1.40 Å long, which is shorter than the length of a single bond (1.47 Å). A triple bond is formed between the two sp -hybridized C atoms in the chain because the length of the C-C bond between them (bond 3) is approximately identical to the length of a triple bond (1.21 Å). The distance between the two nearest hexagonal rings is 4.03 Å.

The C atoms in the hexagonal ring are alternatively replaced by BN atoms, as seen in Fig. 4a, while the other atomic locations are left unaltered. The measured B-N bond (bond 1) length is 1.479 Å, which is longer than the B-N bond length in the original BN sheet (1.452 Å) [44, 45]. The lengths of the C-B bond (bond 2) and C-N atoms (bond 4) are observed to be 1.502 Å and 1.344 Å, respectively. In the linear chain, the bond between C and C atoms (bond 3) is 1.220 Å long, with no change in the triple bond characteristics.

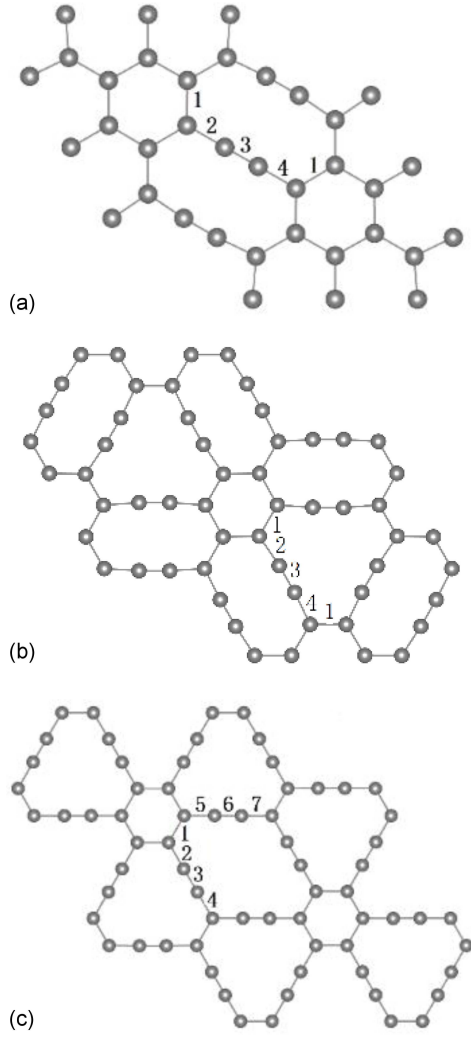


Fig. 5. Bond types of (a) 10-18-6 graphyne, (b) 10-12-18-6 graphyne, and (c) 12-14-18-6 graphyne.

As shown in Fig. 4b, the C–C bond length (bond 1) in the hexagonal ring is decreased to 1.445 Å when the C atoms in the 10-18-6 graphyne linear chain are replaced by BN atoms to achieve doping, and the bond length between the sp^2 -hybridized C atom and B (N) atom is 1.505 Å (1.332 Å). Due to the different radii of the BN atoms, the C–B bond is significantly longer than the C–N bond. The B–N bond (bond 3) in the linear chain is 1.271 Å and is characteristic of a triple bond.

The structure of the BN sheet that resembles 10-18-6 graphyne is now considered (Fig. 4c). Such a system consists of the hybridization of a mixed type ($sp^2 + sp$). The length of the B–N bond in hexagonal rings (bond 1) is found to be 1.461 Å, which is longer than the bond length of the original BN sheet, which is 1.452 Å [42, 43]. In the middle of the linear chain, the chemical bond between the B and N atoms (bond 3) has a triple bond character, and its length is 1.256 Å. The chemical bond

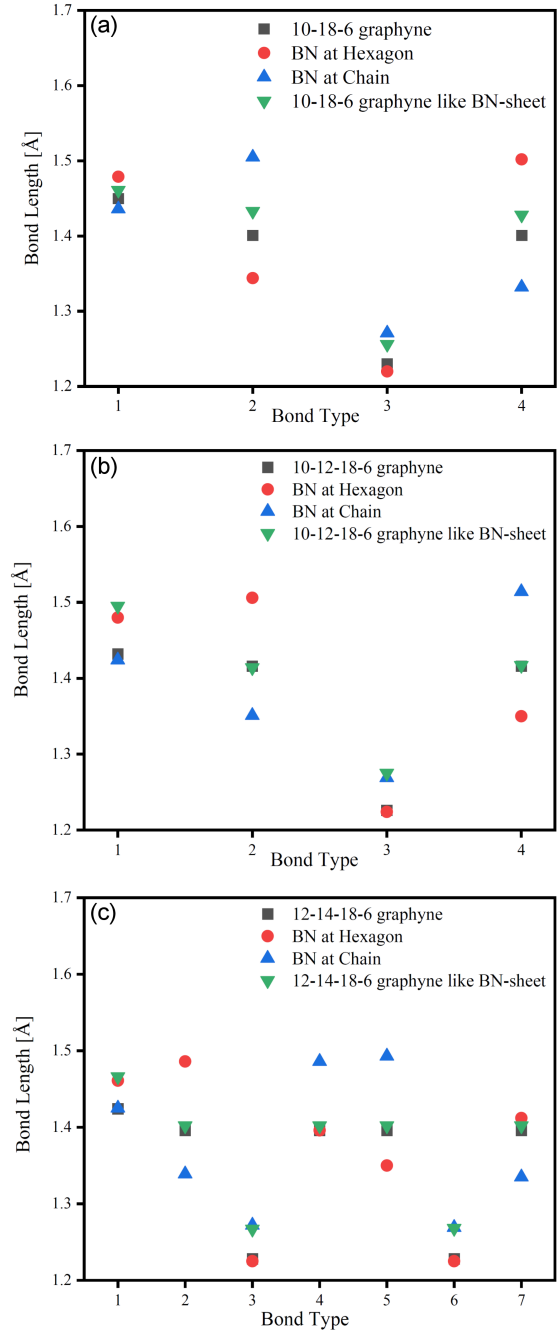


Fig. 6. Bond lengths of (a) 10-18-6 graphyne and its analogues, (b) 10-12-18-6 graphyne and its analogues, and (c) 12-14-18-6 graphyne and its analogues.

between the B atom in the hexagonal ring and the N atom in the linear chain (bond 2) is a B–N bond, and the chemical bond between the B atom in the linear chain and the N atom in the hexagonal ring (bond 4) is also a B–N bond, but they have different lengths, i.e., the former is 1.433 Å long, while the latter is shorter than the former at 1.428 Å. Bond 2 and bond 4 have slightly different bond lengths due to different environments around the B and N atoms. For bond 4, the B atom forms chemical

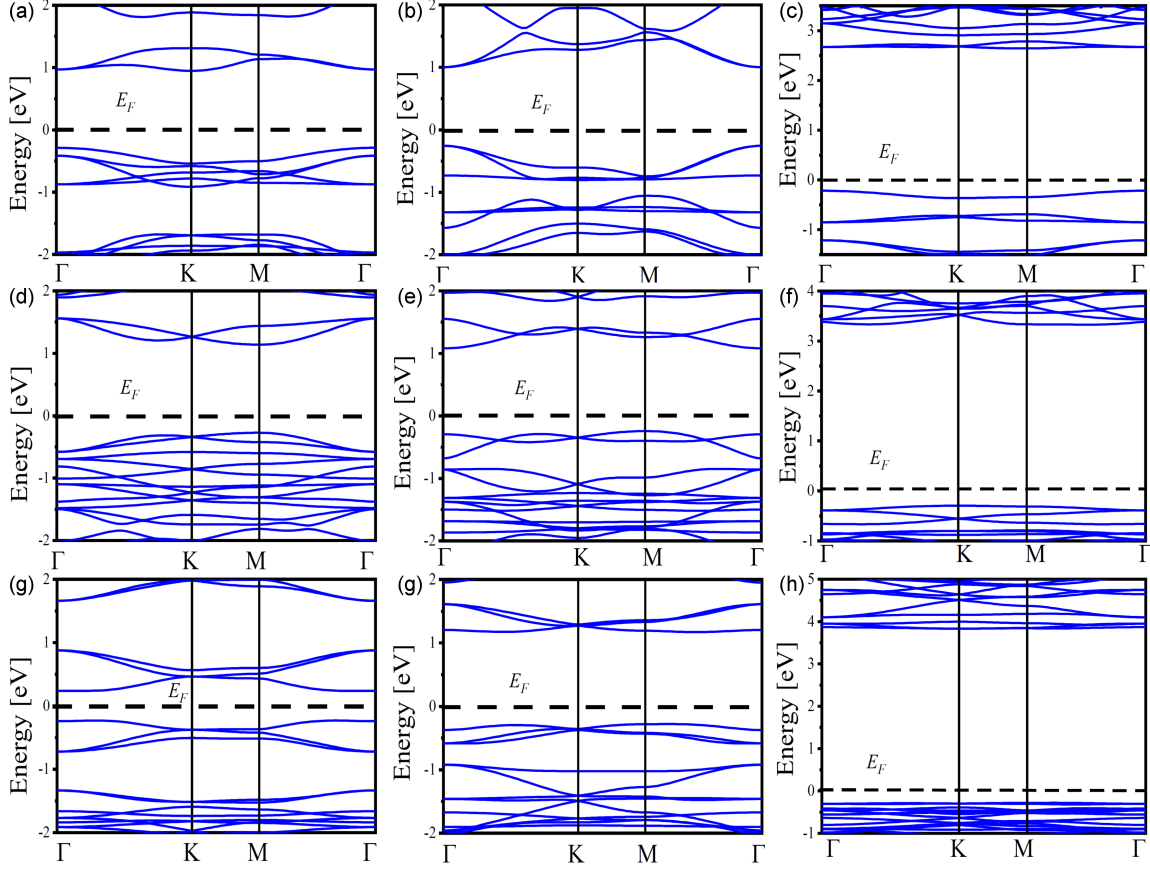


Fig. 7. Band structures of (a) 10-18-6 graphyne with BN in the hexagonal ring, (b) 10-18-6 graphyne with BN in the linear chain, (c) the 10-18-6 graphyne-like BN sheet, (d) 10-12-18-6 graphyne with BN in the hexagonal ring, (e) 10-12-18-6 graphyne with BN in the linear chain, (f) the 10-12-18-6 graphyne-like BN sheet, (g) 12-14-18-6 graphyne with BN in the hexagonal ring, (h) 12-14-18-6 graphyne with BN in the linear chain, and (i) 12-14-18-6 graphyne-like BN sheet.

bonds with three N atoms (one in the chain and two in the hexagonal ring), while in the case of bond 2, only two N atoms (one in the hexagonal ring and the other in the linear chain) are bonded to the B atom.

The comparison of bond lengths before and after doping of the three graphynes is shown in Fig. 6. The hexagonal ring in 10-12-18-6 graphyne has a C–C bond (bond 1) that measures 1.432 Å, which is longer than a typical double C–C bond but shorter than a typical single C–C bond. Bonds 2 and 4 (which join the carbon atoms in the hexagonal ring and the chain) are shorter than the typical single C–C bond, measuring 1.416 Å, whereas bond 3 is almost as long as the triple bond (~ 1.210 Å), measuring 1.226 Å.

The band structures after doping with BN atoms at the hexagonal positions, at the linear positions, and in the overall system were estimated, as shown in Fig. 7a, b, and c. When BN atoms are doped in the hexagonal rings of 10-18-6 graphyne, its band structure (Fig. 7a) reveals that VBM and CBM are positioned at the Γ point and K point, respectively, and that its band gap value (1.235 eV)

is significantly higher than that of 10-18-6 graphyne. Both VBM and CBM are at the Γ point according to the band structure in Fig. 7b, and the band gap increases to 1.258 eV when BN atoms replace carbon atoms at linear chain locations. The band structure of the 10-18-6 graphyne-like BN sheet is shown in Fig. 7c, and it indicates that the indirect band gap of the material is 2.858 eV (VBM is at the Γ point, while CBM is at the M point).

After BN replaces each carbon atom, the band gap becomes very wide compared to the pristine graphyne allotropes (2.858, 3.623, and 4.112 eV for 10-18-6 graphyne, 10-12-18-6 graphyne, and 12-14-18-6 graphyne-like BN sheets, respectively). Therefore, the BN codoping method can provide more flexibility for band gap tuning of these three graphyne allotropes and has the potential to further expand the potential applications of graphyne in optoelectronics.

To evaluate the contribution of different atoms and orbitals, we simultaneously estimated the total density of states (TDOS) and the partial density of states (PDOS).

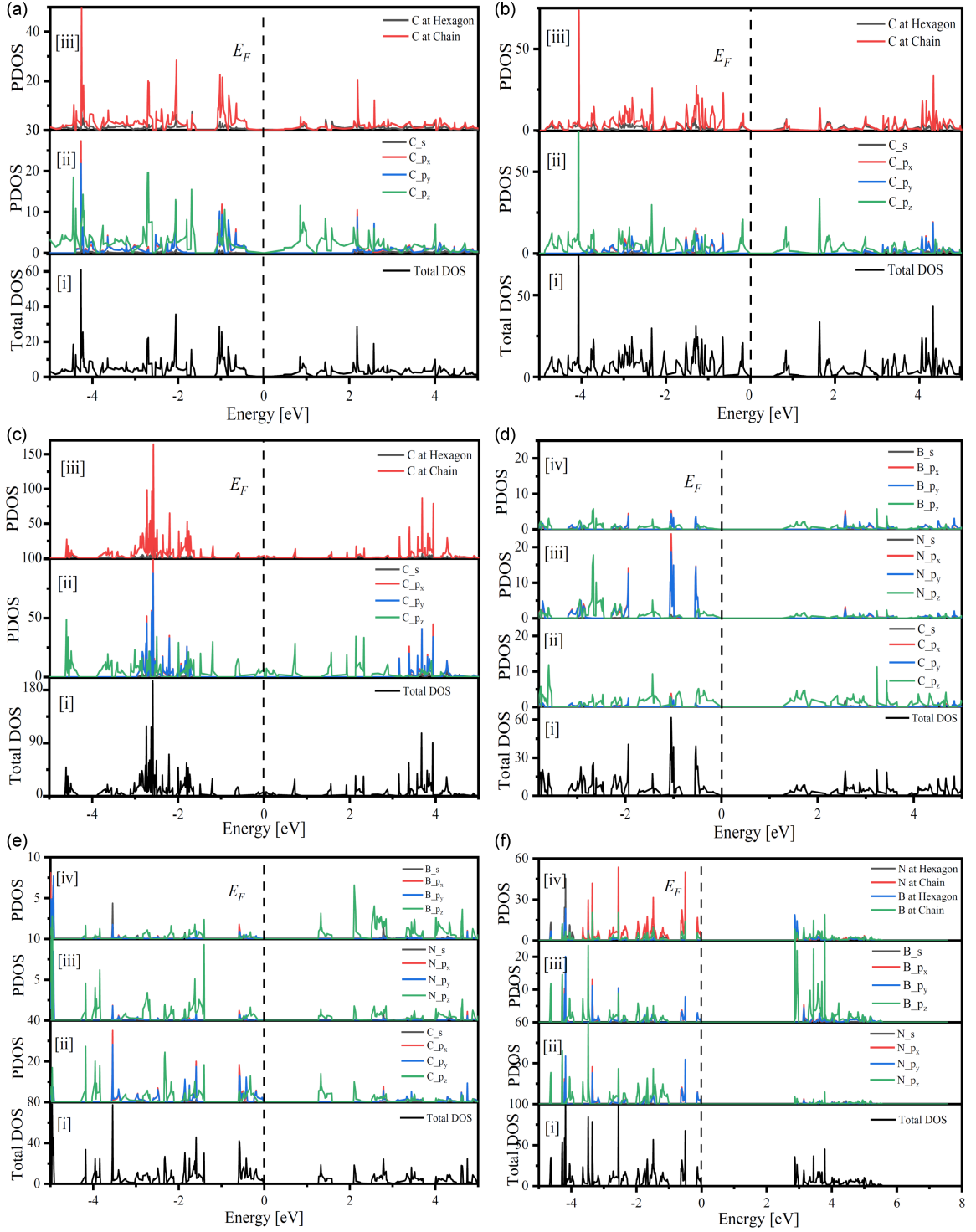


Fig. 8. Total and partial DOS of (a) 10-18-6 graphyne, (b) 10-12-18-6 graphyne, (c) 12-14-18-6 graphyne, (d) 10-18-6 graphyne with BN in the linear chain, (e) 10-18-6 graphyne with BN in the hexagonal ring, and (f) 10-18-6 graphyne-like BN sheet.

The density of states of the 10-18-6 original graphyne is shown in Fig. 8a. The range from -5.000 to -4.379 eV (Fig. 8a(ii)) is primarily contributed by p_z orbitals, whereas the range from -4.379 to -1.573 eV is primarily contributed by p_x , p_y , and p_z orbitals. Notably, the p_z orbital makes a larger

contribution than the p_x and p_y orbitals. The C atom p_z orbital makes the greatest contribution to the conduction band (CB) below 2.065 eV. Orbitals p_x , p_y , and p_z all contribute to the area between 2.065 and 5.0 eV, albeit the p_z orbital contribution occasionally outweighs those of the p_x and p_y

orbitals and vice versa (Fig. 8a(ii)). According to Fig. 8a(iii), both C atoms in the linear chain and C atoms in the hexagonal ring contribute to the area between -5.0 – -4.634 eV and -1.843 – -1.109 eV in the valence band. However, for the areas between -4.634 and -1.843 eV (Fig. 8a(iii)) and between -1.109 and -0.400 eV, the contribution of atoms in the linear chain is dominant. The C atoms at the hexagonal ring sites and the linear sites contribute almost equally to the energy level in the range of 2.673 eV above the Fermi level in the CB area, whereas in the range from -2.673 to -4.322 eV, the C atoms in the linear chain make most of the contribution to the energy level. The contributions from the C atoms at the linear chain position and the hexagonal chain positions are nearly equal in the energy range of 4.322 to 5.000 eV.

The density of states of 10-12-18-6 graphyne is shown in Fig. 8b(ii). The p_z orbital contributes almost all the energy states near the Fermi energy (-0.624 – 3.109 eV), while the s , p_x , and p_y orbitals hardly make any substantial contributions. The primary contributions to the VB energy in the range from -1.561 to -0.624 eV come from the p_x , p_y , and p_z orbitals, whereas the s orbital contribution is minimal. Orbitals p_x , p_y , and p_z all contribute to the energy states in the CB (4.020 – 4.353 eV) area, however the p_z orbital contributes less than the other two orbitals. As can be plainly observed in Fig. 8(b)(iii), the contribution of linear atoms is higher than that of hexagonal ring atoms. It can also be seen by comparing 10-18-6 graphyne and 10-12-18-6 graphyne that linear atoms contribute more than hexagonal ring atoms (see Fig. 8a(iii) and 8b(iii)) because there are more linear chain atoms than hexagonal ring atoms in the whole system.

The density of states of 12-14-18-6 graphyne is depicted in Fig. 8c. In the VB and CB regions of 12-14-18-6 graphyne, the contribution behaviour of the s , p_x , p_y , and p_z orbitals is essentially identical to that for 10-18-6 graphyne and 10-12-18-6 graphyne. The only difference is that the p_x and p_y orbitals contribute more to the energy level near the Fermi level compared to 10-18-6 graphyne and 10-12-18-6 graphyne. In 10-18-6 graphyne and 10-12-18-6 graphyne, the contributions of the s , p_x , and p_y orbitals near the Fermi energy (from -1.647 to 3.117 eV for 12-14-18-6 graphyne) are negligible, and only the p_z orbital contributes in 12-14-18-6 graphyne.

The total density of states and partial density of states of 10-18-6 graphyne doped with BN atoms at the linear chain sites, hexagonal sites, and in the overall system are shown in Fig. 8d, e, and f. The contributions of carbon, nitrogen, and boron atoms are depicted in Fig. 8d(ii), (iii), and (iv)). As seen in Fig. 8d(ii), the p_z orbitals of carbon atoms equally contribute to the VB and CB areas. According to Fig. 8d(iii) and (iv), all p orbitals for nitrogen and boron atoms contribute to both the valence and conduction bands. However, in the case of nitrogen, the p -orbitals contribute more to the total density

of states t in the VB region than to those in the CB region, whereas in the case of boron, we see the opposite contributions. The p_z orbitals of all three atoms contribute to the energy levels on either side of the Fermi level first, in comparison to the other orbitals.

Figure 8e(ii), (iii), and (iv) shows the contributions of a single atom to the density of states when BN atoms take the place of atoms at the hexagonal position in 10-18-6 graphyne. All of the C atom p orbitals contribute to the valence and conduction bands (see Fig. 8e(ii)), while this is not the case when the BN atom is positioned in the linear chain of 10-18-6 graphyne. In Fig. 8d(ii), the p_z orbital of the C atom is the primary contributor to these two bands (see Fig. 8d(ii)). According to Fig. 8e(iii), the contribution of N atoms is mostly from the p_z orbital, with only a small contribution from the p_x and p_y orbitals. As demonstrated in Fig. 8e(iv), the p_z orbital of the B atom contributes significantly more than the other orbitals.

The p orbital of the N atom contributes predominantly to the level near the Fermi level in the VB region of the 10-18-6 graphyne-like BN sheet (Fig. 8f(ii)), whereas the p orbital of the B atom contributes mainly to the level near the Fermi level in the CB region (Fig. 8f(iii)). The p_z orbital contributes more than the other orbitals in both cases, with the p_y orbital first contributing to the valence band close to the Fermi level and the p_z orbital first contributing to the conduction band close to the Fermi level. N atoms are the primary contributors in the valence band area, whereas B atoms are the key contributors in the conduction band region. The N atoms in the linear chain contribute the majority of the N atom contributions to the VB area, whereas atoms at the hexagonal positions contribute only a minor portion (see Fig. 8f(iv)). When the contributions of B atoms near the Fermi level in the CB region are considered, the contributions of B atoms at the linear chain and hexagonal sites are essentially identical (see Fig. 8f(iv)).

4. Conclusions

The geometric structure and electronic characteristics of 10-18-6, 10-12-18-6, and 12-14-18-6 graphynes were comprehensively examined through the BN atom doping method within the context of density functional theory. The band gap is discovered to be connected to the BN atom doping location. The energy levels close to the Fermi energy are more influenced by linear chain atoms than by hexagonal ring atoms in the pristine graphyne system. However, compared to 10-18-6 graphyne and 10-12-18-6 graphyne, the contribution of the 12-14-18-6 graphyne p_x and p_y orbitals begins at levels closer to the Fermi level. When BN atoms replace carbon atoms, the p orbital contribution of nitrogen atoms to VB is greater than that to CB; however, when

boron is the replacement atom, the reverse effect occurs. The N atoms located at linear chain positions contribute more to the VB region than atoms located in hexagonal rings.

Acknowledgments

This work was financially supported by the National Natural Science Foundation of China (Grant Nos.: 11965005 and 11964026), the 111 Project, the Natural Science Basic Research Plan in Shaanxi Province of China (Grant Nos.: 2023-JC-YB-021, 2022JM-035), and the Fundamental Research Funds for the Central Universities. All the authors thank the computing facilities at the High Performance Computing Center of Xidian University.

References

- [1] X. Yang, Y. Wang, R. Xiao, H. Liu, Z. Bing, Y. Zhang, X. Yao, *J. Phys. Condens. Matter* **33**, 045502 (2021).
- [2] X. Wang, Z.H. Feng, J. Rong, Y.N. Zhang, Y. Zhong, J. Feng, X.H. Yu, Z.L. Zhan, *Carbon* **142**, 438 (2019).
- [3] D. Sen, B.K. Das, S. Saha, R. Roy, A. Mitra, K.K. Chattopadhyay, *Carbon* **146**, 430 (2019).
- [4] X.Y. Li, Q. Wang, P. Jena, *J. Phys. Chem. Lett.* **8**, 3234 (2017).
- [5] X.Y. Wu, X.H. Shi, M.G. Yao, S.J. Liu, X.G. Yang, L.Y. Zhu, T. Cui, B.B. Liu, *Carbon* **123**, 311 (2017).
- [6] K.S. Novoselov, A.K. Geim, S.V. Morozov, D. Jiang, Y. Zhang, S.V. Dubonos, I.V. Grigorieva, A.A. Firsov, *Science* **306**, 666 (2004).
- [7] G.X. Li, Y.L. Li, H.B. Liu, Y.B. Guo, Y.J. Li, D.B. Zhu, *Chem. Commun.* **46**, 3256 (2010).
- [8] S. Iijima, *Nature* **354**, 56 (1991).
- [9] Y. Yang, G. Yang, X. Peng, *Appl. Surf. Sci.* **529**, 147150 (2020).
- [10] C. Zhang, Y. Cao, X. Dai, X.Y. Ding, L.L. Chen, B.S. Li, D.Q. Wang, *Nanomaterials* **10**, 816 (2020).
- [11] X.J. Chen, W.X. Xu, B. Song, P.M. He, *J. Phys. Condens. Matter* **32**, 215501 (2020).
- [12] K.S. Novoselov, A.K. Geim, S.V. Morozov, D. Jiang, M.I. Katsnelson, I.V. Grigorieva, S.V. Dubonos, A.A. Firsov, *Nature* **438**, 197 (2005).
- [13] Y.B. Zhang, Y.W. Tan, H.L. Stormer, P. Kim, *Nature* **438**, 201 (2005).
- [14] L.C. Xu, R.Z. Wang, M.S. Miao, X.L. Wei, Y.P. Chen, H. Yan, W.M. Lau, L.M. Liu, Y.M. Ma, *Nanoscale* **6**, 1113 (2014).
- [15] S.H. Cheng, K. Zou, F. Okino, H.R. Gutierrez, A. Gupta, N. Shen, P.C. Eklund, J.O. Sofo, J. Zhu, *Phys. Rev. B* **81**, 205435 (2010).
- [16] M.I. Katsnelson, K.S. Novoselov, A.K. Geim, *Nat. Phys.* **2**, 620 (2006).
- [17] Y.C. Fan, M.W. Zhao, X.J. Zhang, Z.H. Wang, T. He, H.H. Xia, X.D. Liu, *J. Appl. Phys.* **110**, 034314 (2011).
- [18] X.F. Fan, Z.X. Shen, A.Q. Liu, J.L. Kuo, *Nanoscale* **4**, 2157 (2012).
- [19] P. Nath, S. Chowdhury, D. Sanyal, D. Jana, *Carbon* **73**, 275 (2014).
- [20] T.P. Kaloni, R.P. Joshi, N.P. Adhikari, U. Schwingenschlögl, *Appl. Phys. Lett.* **104**, 073116 (2014).
- [21] L. Ci, L. Song, C.H. Jin, D. Jariwala, D.X. Wu, Y.J. Li, A. Srivastava, Z.F. Wang, K. Storr, L. Balicas, F. Liu, P.M. Ajayan, *Nat. Mater.* **9**, 430 (2010).
- [22] M. Zhang, G.Y. Gao, A. Kutana, Y.C. Wang, X.L. Zou, J.S. Tse, B.I. Yakobson, H.D. Li, H.Y. Liu, Y.M. Ma, *Nanoscale* **7**, 12023 (2015).
- [23] B. Xu, Y.H. Lu, Y.P. Feng, J.Y. Lin, *J. Appl. Phys.* **108**, 073711 (2010).
- [24] R.H. Baughman, H. Eckhardt, M. Kertesz, *J. Chem. Phys.* **87**, 6687 (1987).
- [25] D. Malko, C. Neiss, F. Vines, A. Görling, *Phys. Rev. Lett.* **108**, 086804 (2012).
- [26] N. Narita, S. Nagai, S. Suzuki, K. Nakao, *Phys. Rev. B* **58**, 11009 (1998).
- [27] N.B. Singh, B. Bhattacharya, U. Sarkar, *Struct. Chem.* **25**, 1695 (2014).
- [28] X.H. Deng, M. Si, J.Y. Dai, *J. Chem. Phys.* **137**, 201101 (2012).
- [29] X.H. Deng, J. Zeng, M. Si, W. Lu, *Europhys. Lett.* **115**, 27009 (2016).
- [30] Y. Mu, S.D. Li, *J. Mater. Chem. C* **4**, 7339 (2016).
- [31] D. Malko, C. Neiss, A. Görling, *Phys. Rev. B* **86**, 045443 (2012).
- [32] Z.L. Sun, Z.G. Shao, C.L. Wang, L. Yang, *Carbon* **110**, 313 (2016).
- [33] B. Bhattacharya, N.B. Singh, U. Sarkar, *Int. J. Quantum Chem.* **115**, 820 (2015).
- [34] H. Bu, M. Zhao, H. Zhang, X. Wang, Y. Xi, Z. Wang, *J. Phys. Chem. A* **116**, 3934 (2012).
- [35] W.Q. Han, L.J. Wu, Y.M. Zhu, K. Watanabe, T. Taniguchi, *Appl. Phys. Lett.* **93**, 223103 (2008).

- [36] P. Hohenberg, W. Kohn, *Phys. Rev.* **136**, B864 (1964).
- [37] W. Kohn, L.J. Sham, *Phys. Rev.* **140**, A1133 (1965).
- [38] G. Kresse, J. Furthmüller, *Phys. Rev. B* **54**, 11169 (1996).
- [39] G. Kresse, D. Joubert, *Phys. Rev. B* **59**, 1758 (1999).
- [40] P.E. Blöchl, *Phys. Rev. B* **50**, 17953 (1994).
- [41] J.P. Perdew, K. Burke, M. Ernzerhof, *Phys. Rev. Lett.* **77**, 3865 (1996).
- [42] H.J. Monkhorst, J.D. Pack, *Phys. Rev. B* **13**, 5188 (1976).
- [43] T. Ouyang, C. Cui, X. Shi, C. He, J. Li, C. Zhang, C. Tang, J. Zhong, *Phys. Status Solidi RRL* **14**, 2000437 (2020).
- [44] M. Topsakal, E. Akturk, S. Ciraci, *Phys. Rev. B* **79**, 115442 (2009).
- [45] Y. Wang, *Phys. Status Solidi RRL* **4**, 34 (2010).